Jurnal Geofisika (2021) Vol. 19, No. 02 pp. 62-68

Amplitude Variation with Frequency as Direct Hydrocarbon Indicator for Quick Look and Different Insight of Hydrocarbon Delineation

Awal F. Mandong[1,*], Reza P.A. Bekti[1], and Rino I.A. Saputra[1]

[1]Geosoftware
[*]Email: awal.mandong@cgg.com

Submit: 2021-11-20; Revised: 2021-12-25; Accepted: 2021-12-28

Abstract: One of the most common and established techniques to identify hydrocarbon presence is by analyzing the amplitude variation with offset (AVO) utilizing the pre-stack seismic data. However, the gather data quality even the availability of pre-stack data could often become an issue. When the seismic wave propagates through a highly attenuating medium (i.e. hydrocarbon-bearing reservoir), it loses its high-frequency content and the dominant frequency tends to slide to the lower frequency. These high-frequency loss phenomena can be used to delineate hydrocarbon-bearing reservoirs using the spectral decomposition method. The continuous wavelet transform (CWT) is used to decompose the seismic and generate the frequency gather data to analyze the frequency loss due to hydrocarbon presence using gradient analysis. The result from this study shows that the hydrocarbon-bearing zone correlates to the high attenuation can be delineated using the Amplitude Variation with Frequency (AVF) analysis method. The hydrocarbon anomaly observed from the AVF analysis result is aligned with the AVO analysis and validated by the water saturation log. The results of this study suggest that AVF analysis method can help to identify as a quick look approach and provide a better confidence level as a direct hydrocarbon indicator when combined with other direct hydrocarbon indicator methods such as the AVO method.
Keywords: Frequency gather, amplitude variation with frequency, AVF, spectral decomposition, time-frequency analysis

Abstrak: Salah satu metoda yang paling umum untuk mengidentifikasi keberadaan hidrokarbon adalah dengan menganalisis perubahan amplitudo terhadap offset (AVO) menggunakan data seismik pre-stack. Namun, kualitas data bahkan ketersediaan data seismik pre-stack sering kali menjadi masalah. Ketika gelombang seismik merambat melalui media yang sangat atenuatif (yaitu reservoir yang mengandung hidrokarbon), gelombang seismik tersebut kehilangan konten frekuensi tinggi dan frekuensi dominan cenderung bergeser ke frekuensi yang lebih rendah. Fenomena kehilangan frekuensi tinggi ini dapat digunakan untuk mendeteksi keberadaan reservoir yang mengandung hidrokarbon menggunakan metode dekomposisi spektral. Continuous Wavelet Transform (CWT) digunakan untuk menguraikan seismik dan menghasilkan data frequency gather untuk menganalisis kehilangan frekuensi karena keberadaan hidrokarbon menggunakan analisis gradien. Hasil dari penelitian ini menunjukkan bahwa zona hidrokarbon yang berkorelasi dengan atenuasi tinggi dapat dideteksi menggunakan metode analisis Amplitude Variation with Frequency (AVF). Anomali hidrokarbon yang diamati dari hasil analisis AVF sejalan dengan analisis AVO dan divalidasi dengan log saturasi air. Hasil penelitian ini menunjukkan bahwa metode analisis AVF dapat membantu untuk mengidentifikasi sebagai pendekatan quick look dan memberikan tingkat kepercayaan yang lebih baik sebagai indikator hidrokarbon langsung bila dikombinasikan dengan metode indikator hidrokarbon langsung lainnya seperti metode AVO.
Kata kunci: Frekuensi, variasi amplitudo terhadap frekuensi, dekomposisi spektrum, analisis waktu-frekuensi

1 INTRODUCTION

The location of the study area is Amberjack Block 109 that located in the Gulf of Mexico (GOM). The depositional environment in this study area is two vertically stacked shelf-edge delta system in the middle of Pliocene of Mississippi Canyon Block 109 as proposed by Mayall, Yeilding, Oldroyd, Pulham, and Sakurai (1992). The shelf-edge area consists of slumps, turbidites, prograding sandy mouth bar and relatively undeformed upper slope area. The slumps themselves are not developed to the same extent in all available wells.

The two deltas are separated by a 152 m section that is dominated by mud. Both upper and lower delta have, approximately, 122 m thick. Latimer and Van Riel (1996) derived the reservoir zones into five which are Orange, Purple, Red, Green, and Blue. The two main reservoirs are Blue and Green while the secondary reservoir zones are Purple, Orange and Red as shown in Figure 1. The Orange and Purple package contains thin sands but covers a large area. The ratios of sand/shale are lower in the turbidite packages and the boundaries are not clear. Another thin reservoir is Red zone that the sedimentary setting is low-density grain flows (turbidity deposits). The first main reservoir is the Green zone that has sand package deposited as overlapping packages of clinoforms in a prograding shelf margin deltaic sequence. Both stratigraphic and structural components are present in this zone as it is partially fault-controlled and the reservoir is continuous wherever the sands overlap. The Blue zone in the lower delta has a prograding package of

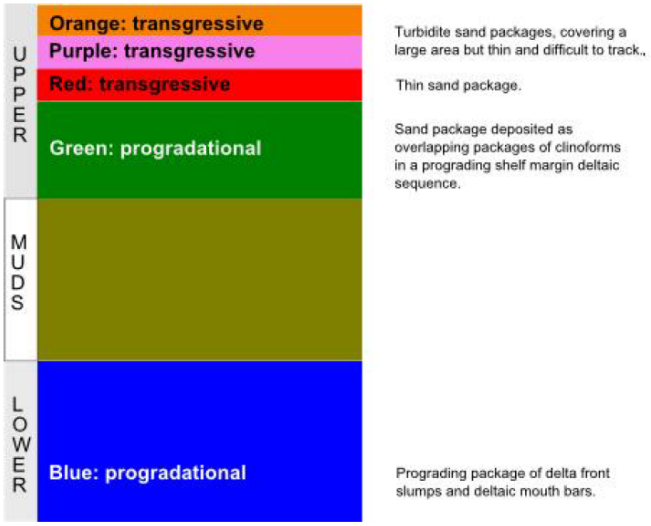

Figure 1. Two vertically stacked shelf-edge delta system that separated by thick mud. The reservoir consits of five zones; Orange, Purple, Red, Green and Blue.

delta front slumps and deltaic mouth bars. This zone has more distinct sand lenses and is separated by larger shale interbeds.

The two vertically stacked shelf-edge show an indication of bright amplitude/bright spot in the post-seismic data. The bright amplitude / bright spot shows high impedance contrast, and the contrast can be caused by various reasons. Meanwhile, the amplitude spectrum more likely shows energy loss represented by decreasing high-frequency content, in other words, it is related to attenuation and velocity dispersion. The factor of geometrical spreading, scattering, and intrinsic attenuation are the reasons why there is seismic amplitude loss. Batzle, Han, and Castagna (1996) shows that rock/fluid interactions are strongly related to intrinsic attenuation and can be an indicator of potential hydrocarbon or permeability.

The observed difference in frequency content between hydrocarbon and non-hydrocarbon as shown in Figure 2 suggests that the hydrocarbon-bearing zone has higher attenuation (green) indicated by lower dominant frequency and lower high-frequency content while the non-reservoir zone has lower attenuation (blue) indicated by higher dominant frequency and high-frequency content. A simple regression line is plotted from approximately the peak of amplitude spectrum to the higher frequency side of each zone. The high attenuation zone has a higher intercept and gradient while the low attenuation zone has a lower intercept and gradient. The intercept and gradient term from AVF method should not be confused with the intercept and gradient from AVO method. The intercept and gradient in the AVO method is representing the amplitude change along with offset or angle while the intercept and gradient in the AVF method is representing the energy of high frequency beyond the peak or dominant frequency.

2 DATA AND METHODOLOGY

The area of study is a 3D seismic survey with an area of around 44 km2 and a record length is 5 seconds. The area of interest is limited from the Orange horizon as the top of the upper delta to the Deep horizon as the base of the lower delta. The migrated full-stack seismic data have been resampled to 4ms and stacked from 0-40 degrees. The dominant frequency content is around 32 Hz which is calculated within the area of interest from -100 ms above Orange horizon to +100 ms below Deep horizon. Although the area of interest is limited to the top of the upper delta and base of the lower delta, the process of generating AVF volume is performed for the whole interval. In general, the process is divided into 4 stages which are performing spectral decomposition, creating frequency gather, evaluating amplitude variation with frequency analysis at well locations, and generating intercept and gradient volume from the frequency gather.

2.1 Spectral Decomposition

The process of spectral decomposition is performed first to create a series of constant frequency amplitude volumes. The application of spectral decomposition is commonly used to map stratigraphy features such as channels, one example is from Mulyani et al. (2018). Conceptually, the spectral decomposition method decomposes the amplitude spectrum of traces over an amplitude spectrum of the different wavelets. Thus, it will be possible to analyze the spectrum for individual frequency, unlike conventional Fourier transform which computes the stationary spectrum of a seismic signal. Unlike the short-time Fourier Transform that limits the technique's temporal resolution by using a fixed time window, the Wavelet Transform utilizes a variable window size (Sinha, Routh, Anno, & Castagna, 2005; Sun, Castagna, & Siegfried, 2002; Xia, 1998). Regarding this aspect, the length of Wavelet Transform is proportional to center frequency that makes both narrowband ringing and broadband impulsive reflections can be analyzed and positioned better in time. The Wavelet Transform decomposes a signal s(t) by the following equation:

$$W(a,\tau) = \frac{1}{\sqrt{a}} \int_{-\infty}^{\infty} S(t)\psi * (\frac{t-\tau}{a})dt \qquad (1)$$

Where ψ is the complex conjugate of the mother wavelet and τ is the time shift applied to the mother wavelet, which is also scaled by "a" (Herrera, Han, & van der Baan, 2014). Wavelet Transform takes the inner product of the input seismic signal, then is compared to a mother wavelet. The wavelet transform has denser frequency sampling at a lower frequency than at a higher frequency due to the logarithmic nature of mother wavelet.

The continuous wavelet transform can generate different outputs such as dominant frequency, constant frequency amplitude, constant phase amplitude, etc. In this study, we output the series of constant frequency amplitude volume from the spectral decomposition method to visualize and analyze the frequency spectrum on each time interval.

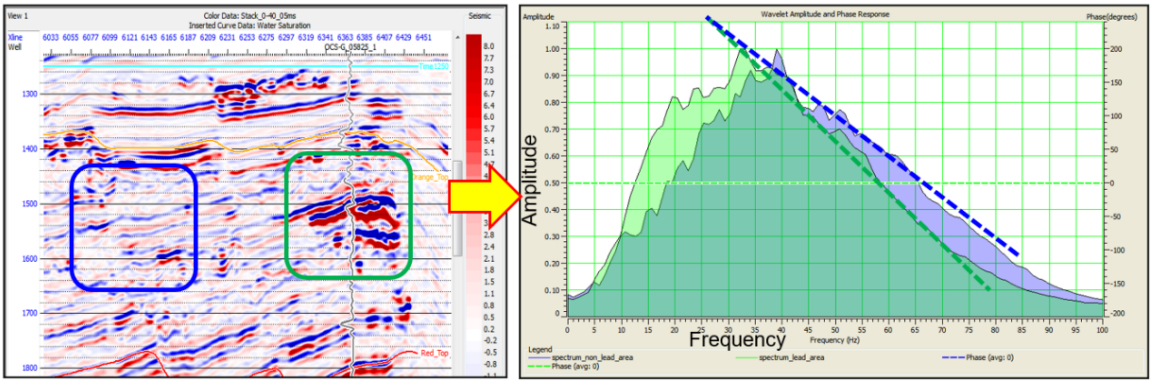

Figure 2. Frequency spectrum; low attenuation zone (blue) and high attenuation zone (green)

2.2 Frequency Gathers

The constant frequency amplitude volumes from spectral decomposition results were sorted into frequency gathers before the amplitude variation with frequency (AVF) analysis shown in Figure 3 and 4. By sorting the data into frequency gather, the analysis of high-frequency loss (attenuation) can be performed at certain seismic traces. This is also done to help interpret the gradient of frequency over a certain frequency range.

2.3 Amplitude Variation with Frequency (AVF)

As the seismic wave propagates from the surface into the subsurface, it loses the high-frequency content as the time increases due to cumulative attenuation. This phenomenon can be observed as decreasing frequency bandwidth and dominant frequency shift, as shown by the black and gray dashed lines in Figure 5. In the attenuating zone (i.e. due to the hydrocarbon presence), the amplitude spectrum at a particular zone or interface tends to have lower dominant frequency and lower high-frequency content relative to the background trend. This anomaly can be used to delineate the hydrocarbon-bearing reservoir. The hydrocarbon-bearing reservoir (annotated by the red arrow in Figure 5) shows lower dominant frequency and lower high-frequency content compared to the trend and the lower zone (annotated by the blue arrow in Figure 5).

From the frequency spectrum, we can draw a line that fits the curve from frequency 30 Hz to 70 Hz using the equation as follow:

$$y = I + G.\sin^2(x) \tag{2}$$

where I = Intercept and G = Gradient along with frequency x To simplify the regression fitting with existing intercept gradient analysis, the AVO gradient analysis from two-terms Aki – Richard equations was used on each time sample of the frequency gather to obtain AVF intercept (I) and gradient (G) as the implementation of this equation is commonly available in advanced seismic interpretation software. The gradient (G) represents frequency spectrum slope, while the intercept (I) represents amplitude which correlates to a bright spot. The gradient value was used to measure attenuation qualitatively relative to the trend or nearby traces. The selection of frequency range to generate the intercept and gradient was performed by analyzing the frequency spectrum over certain intervals around the target zone to avoid pitfall due to the significant frequency content difference over a long interval or different trend.

2.4 Generating Intercept and Gradient from Frequency Gather

A total of five wells were used in the AVF analysis, and the water saturation log was used to validate the hydrocarbon presence around the well location. The AVF analysis results (Intercept (I) and Gradient (G)), were multiplied to delineate bright spots with high relative attenuation. The AVO product (AVO I*G) was used as a comparison of two methods with different approaches. This is considering where AVF analysis is based on frequency signature while AVO is based on amplitude change along with offset or angle.

3 RESULTS AND DISCUSSIONS

In general, the AVF anomaly is consistent with the AVO anomaly, showing good validation around well location using water saturation log as shown in Figure 6. One limitation of the AVF result is the resolution degradation as spectral decomposition represents the energy of each generated frequency similar to the amplitude envelope where all the amplitudes are positive. Therefore, the seismic resolution over a peak-trough separation no longer can be observed. On the other hand, the AVO analysis compares the amplitude along with offset or angle where the gather quality (i.e. the presence of noise and misalignment) becomes a major issue. The impact of poor gather quality appears as noisy AVO product and thinner events compared to the seismic itself as shown in the Figure 6. The multiplication of intercept and gradient from AVF is expected to work as a hydrocarbon indicator, similarly like the AVO Product. Comparison between the AVO product and AVF product are shown at Figure 6, and the result of AVF workflow is quite close to the conventional AVO approach, this can be seen on the right image in Figure 6.

A Lambda-Rho volume as quantitative analysis result was used as it has sensitivity to fluid content. In this

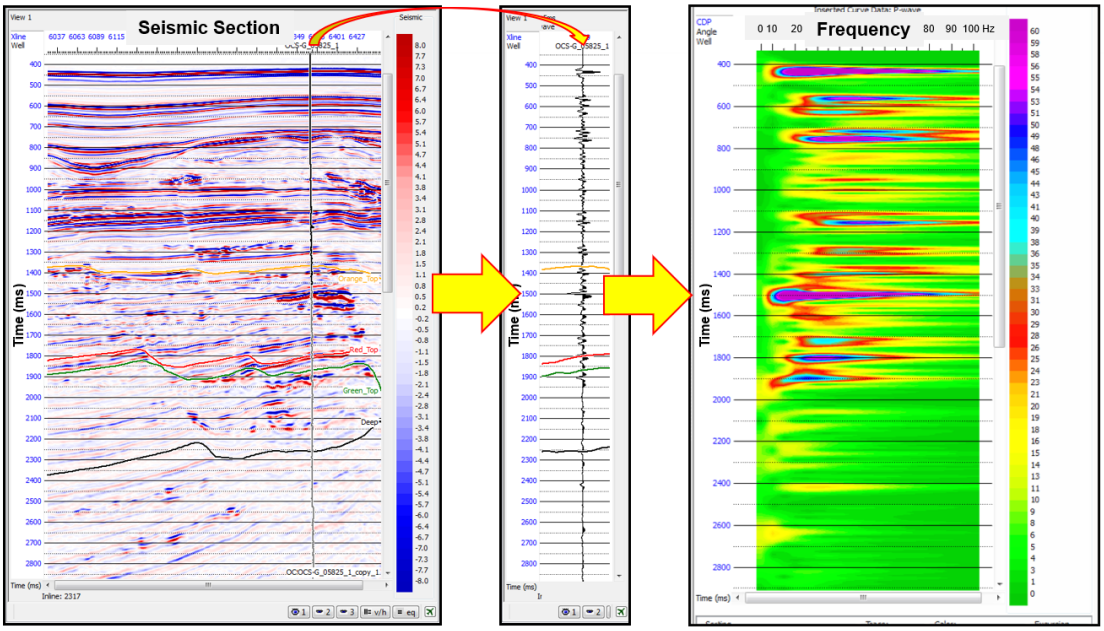

Figure 3. The spectral decomposition method decompose each trace of seismic data to a frequency gather.

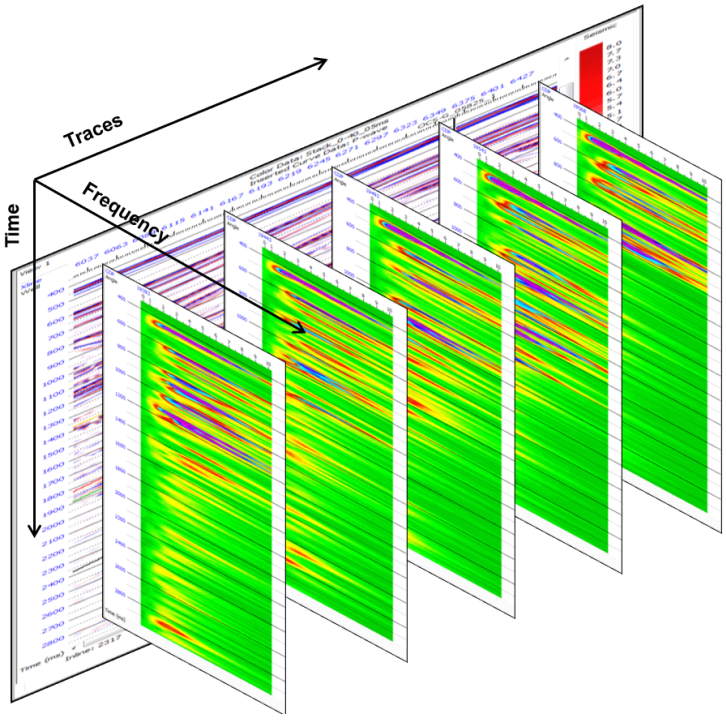

Figure 4. The spectral decomposition generate output data with one dimension larger than the input data.

study, Lambda-Rho were generated by first doing simultaneous inversion from available partial stacks to produce P-Impedance and Shear Impedance which were then used to derive Lambda-Rho. The importance of Lambda-Rho in this study is to be used as a benchmark on the AVF approach. Figure 7 shows the AVF anomaly which is overlaid on post-stack seismic and Lambda-Rho as comparison. The AVF anomaly shows consistentcy with the low Lambda-Rho which generally represents low incompresibility which could relate to hidrocarbon presence. The mean amplitude slice was extracted from Green horizon to 50 ms below green horizon on AVF, AVO, and Lambda-Rho volume. the AVF anomaly is generally consistent with the AVO anomaly and low Lambda-Rho area as shown in Figure 8.

Figure 8 shows the mean amplitude slice within 100 ms interval around Green horizon between I*G from AVF, I*G from AVO and Lambda-Rho result. In general, the trend of anomaly among these results are aligned with each other. For AVO and AVF result is a quite close in capturing the trend of anomaly, and some of different anomalies are due to the resolution of these two methods. However, the area of AVO and AVF slice that has difference to Lambda-Rho slice is in the area around Well-4, and this is due to the product of simultaneous inversion which can quantify the property better.

4 CONCLUSIONS

In this case study, the combined analysis of frequency loss phenomena and spectral decomposition has been used to detect hydrocarbon presence. The amplitude versus frequency (AVF) analysis can be used as a direct hydrocarbon indicator when pre-stack data is not available or as additional information to the hydrocarbon detection using conventional AVO analysis. As the AVO is sensitive to gather quality, sometimes some anomaly is failed to be delineated when the seismic gather is noisy or not properly aligned. Meanwhile, since the AVF analysis utilize the post-stack data, it does not exhibit issue due to gather quality such as noise and alignment. The AVF analysis also give the advantages when the data has been applied with AVO harming process during seismic processing. Utilizing both AVF and AVO analysis helps to reduce uncertainty and minimizing risk in hydrocarbon delineation.

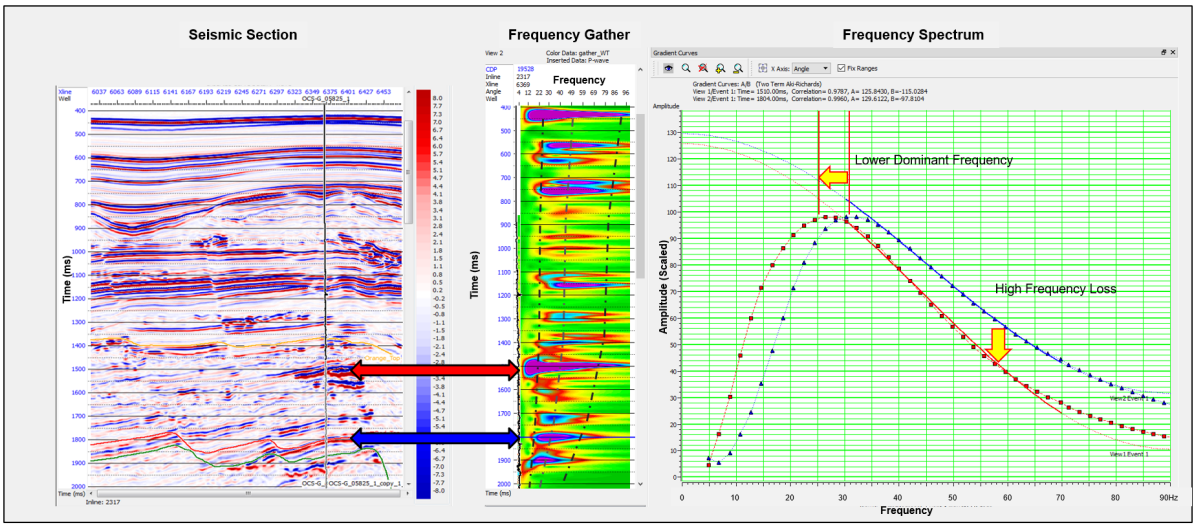

Figure 5. Seismic section (left), frequency gather in color mode (middle), and frequency plot on the two time events annotated by red and blue arrow (right).

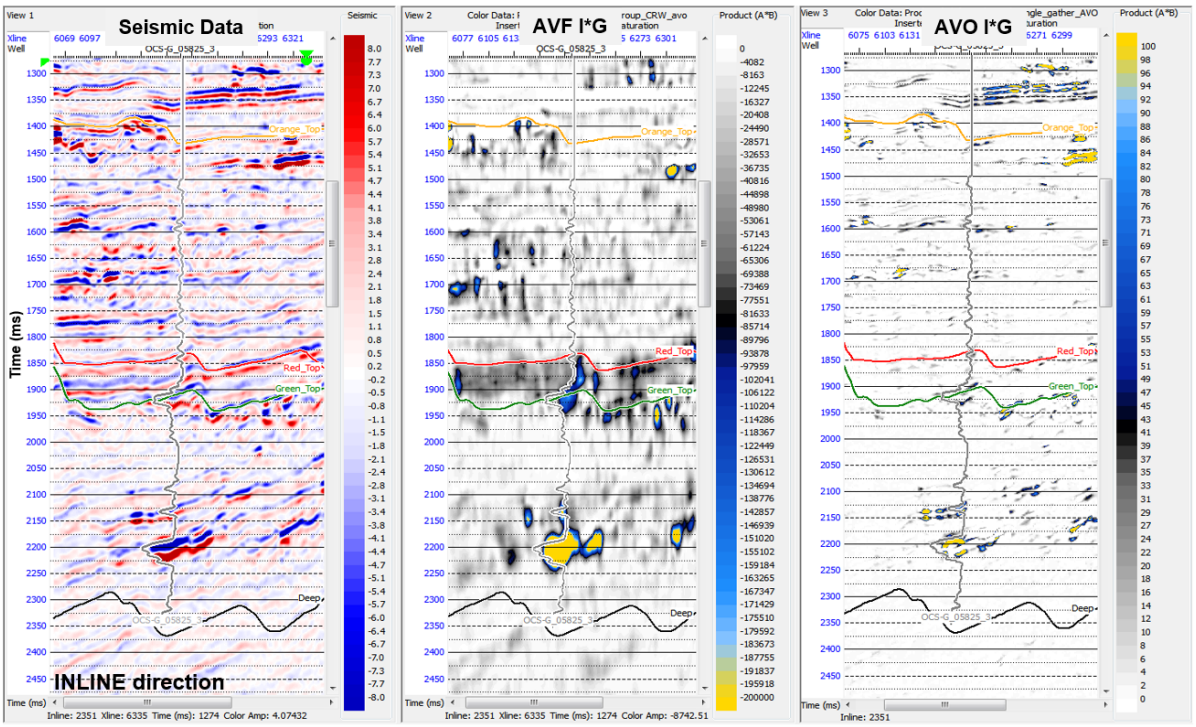

Figure 6. Section of post-stack seismic data (left), I*G from AVF (middle), and I*G from AVO (right). The AVF anomaly shows consistency with the AVO anomaly and Sw log at the well location

ACKNOWLEDGMENTS

The authors wish to thank Stone Energy for permission to show these data. They also thank their colleagues in the GeoSoftware Far East team for their valuable comments and support.

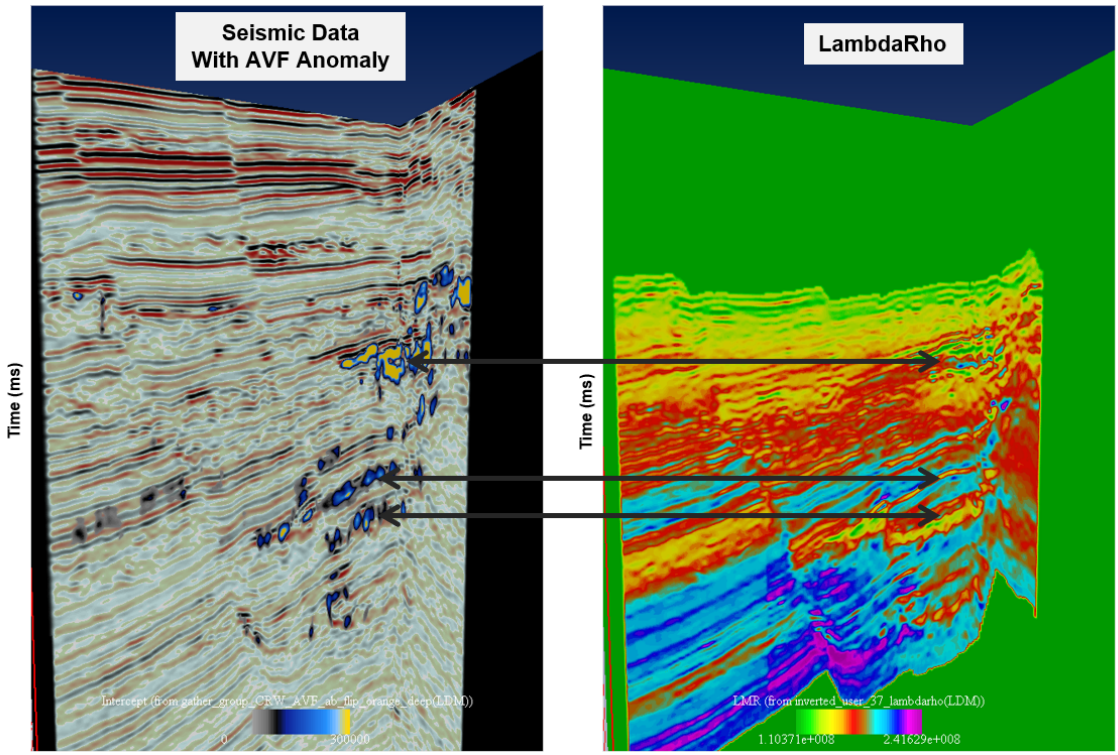

Figure 7. The AVF anomaly overlaid on post-stack seismic (left)and lambda-rho (right) as comparison. The AVF method shows anomaly consistent with the low lambda-rho which represents low incompresibility related to hidrocarbon presence.

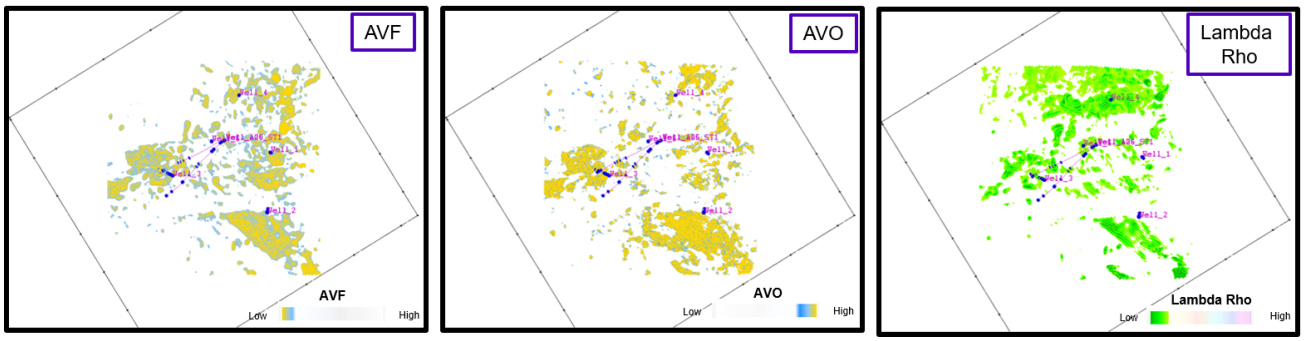

Figure 8. Mean amplitude slice of I*G from AVF (left), I*G from AVO (right), and Lambda-Rho (bottom) within 50 ms interval below Green horizon. The AVF anomaly generally shows consistency with the AVO anomaly and Lambda-Rho.

References

Batzle, M., Han, D.-h., & Castagna, J. (1996). Attenuation and velocity dispersion at seismic frequencies. In *Seg technical program expanded abstracts 1996* (pp. 1687–1690). Society of Exploration Geophysicists.

Herrera, R. H., Han, J., & van der Baan, M. (2014). Applications of the synchrosqueezing transform in seismic time-frequency analysis. *Geophysics*, *79*(3), V55–V64.

Latimer, R. B., & Van Riel, P. (1996). Integrated seismic reservoir characterization and modeling: A gulf of mexico 3d case history.

Mayall, M., Yeilding, C., Oldroyd, J., Pulham, A., & Sakurai, S. (1992). Facies in a shelf-edge delta—an example from the subsurface of the gulf of mexico, middle pliocene, mississippi canyon, block 109. *AAPG bulletin*, *76*(4), 435–448.

Mulyani, R., Widiatmo, R., Gunawan, H., Nugroho, Hairunnisa, Mandong, A., & Saputra, R. (2018). New approach: Using relative inversion with spectral decomposition to distinguish thin layers in the 33-series sand reservoirs of the widuri field, southeast sumatra, indonesia.

Sinha, S., Routh, P. S., Anno, P. D., & Castagna, J. P. (2005). Spectral decomposition of seismic data with continuous-wavelet transform. *Geophysics*, *70*(6), P19–P25.

Sun, S., Castagna, J. P., & Siegfried, R. W. (2002). Examples of wavelet transform time-frequency analysis in direct hydrocarbon detection. In *Seg technical program expanded abstracts 2002* (pp. 457–460). Society of Exploration Geophysicists.

Xia, X.-G. (1998). A quantitative analysis of snr in the short-time fourier transform domain for multicomponent signals. *IEEE Transactions on Signal Processing*, *46*(1), 200–203.